BJRS

BRAZILIAN JOURNAL
OF
RADIATION SCIENCES
09-02B (2021) 01-15

Simulation of transients in ads reactors in three-dimensional geometry

José Rafael Nicolao Carneiro, Zelmo Rodrigues de Lima, Alessandro da Cruz Gonçalves

Instituto de Engenharia Nuclear (IEN / CNEN - RJ)

jrnc@hotmail.com

ABSTRACT

Accelerator-Driven System, ADS, belong to the new generation of advanced reactors being developed that promise to drastically reduce the life of radioactive waste by, for example, the transmutation process. Subcritical reactor designs of the ADS type have attracted worldwide attention and are the subject of research and development in several countries. The purpose of this work is to simulate transients associated with ADS. It adopted the neutron diffusion model that leads the spatial kinetics equations. These equations are solved by the known numerical method of finite differences. The simulations are performed considering transients related to the variations in the intensity of the proton flux provided by the particle accelerator acting in a sub-critical reactor in three-dimensional geometry for two energy groups and six groups of delayed neutron precursors.

Keywords: subcritical core, spatial kinetics, transients.

ISSN: 2319-0612
Accepted: 2021-05-28

1. INTRODUCTION

Although nuclear power is the best choice of renewable energy sources for clean energy production without polluting the environment, its use is still associated with some impasses in society related to past radiological and nuclear accidents. When an accident occurs, the related safety issues are reviewed, and mandatory improvements and new safety protocols are implemented to ensure that the same problems never happen again, making thermonuclear plants increasingly safe. Another obstacle to nuclear energy is the community's acceptance of the final destination of spent fuel due to the risk of proliferation of nuclear weapons and the costly form of safe storage of spent fuel.

Concern about used fuel can still be minimized if it is better utilized. That is precisely the proposal of the Accelerator Driven Subcritical Nuclear Reactor (ADSR), also known as Hybrid Reactor [1] because it works simultaneously with a high energy proton accelerator, which strikes a heavy metal in the center of core, causing the phenomenon of spallation and producing excess neutrons, which can be used to transmute and incinerate the part that requires greater attention from the spent fuel.

The purpose of this work is to study the behavior of the ADS reactor by analyzing transients caused by postulated accelerator malfunction using spatial kinetics equations in three dimensions, giving continuity to the study developed in previous works [2], [3], [4] , [5].

In order to test the numerical method, a computer code programmed in FORTRAN language was implemented. The code solves equations of spatial kinetics with or without external neutron source in three-dimensional geometry for two energy groups and up to six groups of precursors. In addition, another computational code was developed to solve the diffusion equation for the steady-state problem with or without external source of neutrons in three-dimensional geometry for two energy groups, providing the steady-state neutron fluxes and the multiplication factor, allowing the analysis of the core sub-criticality level.

2. ACCELERATOR-DRIVEN SUBCRITICAL KINETICS

The three-dimensional spatial kinetic neutron diffusion equations, for two energy groups, six delayed neutron precursor groups and with the presence of an external source are written as follows:

$$\frac{1}{\upsilon_g}\frac{\partial}{\partial t}\phi_g(\vec{r},t) - D_g\nabla^2\phi_g(\vec{r},t) + \Sigma_{Rg}\phi_g(\vec{r},t) = \sum_{\substack{g'=1 \\ g'\neq g}}^{2}\Sigma_{sgg'}\phi_{g'}(\vec{r},t) +$$
$$+ \chi_{P,g}(1-\beta)\sum_{g'=1}^{2}\nu\Sigma_{fg'}\phi_{g'}(\vec{r},t) + \sum_{l=1}^{6}\chi_{D,l}\lambda_l c_l(\vec{r},t) + \mathrm{S}_{\mathrm{es,g}}(\vec{r},t) \ , \mathrm{g} = 1 \mathrm{e}\ 2 \tag{1}$$

$$\frac{\partial}{\partial t}c_l(\vec{r},t) = -\lambda_l c_l(\vec{r},t) + \beta_l\sum_{g'=1}^{2}\nu\Sigma_{fg'}\phi_{g'}(\vec{r},t) \ , \ \ell = 1,...,6 \tag{2}$$

where for each energy group g, $\phi_g(\vec{r},t)$ is the neutron flux, D_g the diffusion coefficient, Σ_{Rg} the removal cross section, $\nu\Sigma_{fg}$ is the average number of neutrons emitted by fission multiplied by fission cross section, $\Sigma_{sgg'}$ the scattering cross section, $\mathrm{S}_{\mathrm{es,g}}(\vec{r},t)$ the external source, defined in the group g of energy, $c_l(\vec{r},t)$ the delayed neutron precursor concentration in precursor group l, all defined at point $\vec{r}$ and time *t*, υ_g the velocity, $\chi_{P,g}$ the fission spectrum for prompt neutrons, both in group g, $\chi_{D,l}$ the fission spectrum for delayed neutrons of the lth group, λ_l the delayed neutron precursor decay constant, β_l the fraction of all fission neutrons emitted per fission, defined in the l precursor group and finally β the total fraction of fission neutrons which are delayed. Equations (1) and (2) are discretized in space and time, as described in the following subsections.

2.1. Spatial Discretization

The spatial discretization scheme adopted is based on classical formulation of finite differences, implemented in the box schema [6], [7]. Therefore, Equations (1) and (2) can be rewritten in the following matrix form:

$$[\upsilon]^{-1}\frac{d}{dt}\underset{\sim}{\Phi}(t) = -\left[B(t)\right]\underset{\sim}{\Phi}(t) + (1-\beta)\left[F(t)\right]\underset{\sim}{\Phi}(t) + \left[S(t)\right]\underset{\sim}{\Phi}(t) + \underset{\sim}{\mathrm{S}}_{es}(t) + \sum_{l=1}^{6}\lambda_l\underset{\sim}{c}_l(t) \tag{3}$$

$$\frac{d}{dt}\underset{\sim}{c}_l(t) = \beta_l\left[F(t)\right]\underset{\sim}{\Phi}(t) - \lambda_l\underset{\sim}{c}_l(t) \tag{4}$$

where

$$[B(t)]=\begin{bmatrix} B_1(t) & 0 \\ 0 & B_2(t) \end{bmatrix},\ [F(t)]=\begin{bmatrix} F_{11}(t) & F_{12}(t) \\ 0 & 0 \end{bmatrix},\ [S(t)]=\begin{bmatrix} 0 & 0 \\ S_{21}(t) & 0 \end{bmatrix}, \tag{5}$$

where [B(t)] is a block-hepta-diagonal matrix operator representing the leakage and removal of neutrons, [F(t)] represents the fission matrix for $\chi_{P,1}=1$ and $\chi_{P,2}=0$, composed of two diagonal blocks, [S(t)] represents the scattering matrix, without considering the upscattering, formed by a diagonal block, and

$$\underset{\sim}{\Phi}(t)=\begin{bmatrix} \underset{\sim}{\phi}_1(t) \\ \\ \underset{\sim}{\phi}_2(t) \end{bmatrix}, \underset{\sim}{\phi}_g(t)=\begin{bmatrix} \phi_g^1(t) \\ \vdots \\ \phi_g^N(t) \end{bmatrix},\ \underset{\sim}{S}_{es}(t)=\begin{bmatrix} \underset{\sim}{S}_{es,1}(t) \\ \\ \underset{\sim}{S}_{es,2}(t) \end{bmatrix}, \underset{\sim}{S}_{es,g}(t)=\begin{bmatrix} S_{es,g}^1(t) \\ \vdots \\ S_{es,g}^N(t) \end{bmatrix}, g=1,2,\quad \underset{\sim}{c}_l(t)=\begin{bmatrix} C_l^1(t) \\ \vdots \\ C_l^N(t) \end{bmatrix}, \tag{6}$$

$$l=1,\ldots,6$$

with *N* being the total number of boxes. The system equations (3) and (4) stands for the semi-discretized form.

2.2. Time Dependent Solution

In order to solve the time dependent equation system, the analytical integration procedure [8] has been adopted for the delayed neutron precursor concentration equation, Equation (4), whereas the Methods Implicit Euler [9] is considered for the neutron flux in Equation (3).

2.2.1. Analytical solution of the delayed neutron precursor equation

In the analytical integration, it was assumed that the fission rate term varies linearly between times t_τ to $t_{\tau+1}$ in equation (4), which was analytically integrated in this interval, thus obtaining the expression for $\underset{\sim}{c}^l(t)$ in $t_{\tau+1}$:

$$\underset{\sim}{c}_l^{(\tau+1)}=\underset{\sim}{c}_l^{(\tau)}e^{-\lambda_l\Delta t}+\beta_l\left\{a_l\sum_{g=1}^{2}F_{1g}\underset{\sim}{\phi}_g^{(\tau)}+b_l\sum_{g=1}^{2}F_{1g}\underset{\sim}{\phi}_g^{(\tau+1)}\right\} \tag{7}$$

where coefficients a_l and b_l are defined as:

$$a_l=\frac{(1+\lambda_l\Delta t)(1-e^{-\lambda_l\Delta t})}{\lambda_l^2\Delta t}-\frac{1}{\lambda_l}\ ,\ \ b_l=\frac{\lambda_l\Delta t-1+e^{-\lambda_l\Delta t}}{\lambda_l^2\Delta t}\ \text{and}\ \Delta t=t_{\tau+1}-t_\tau\ . \tag{8}$$

2.2.2. Implicit Euler

The implicit Euler method applied to the matrix equation, Equation (3), leads to the following expression:

$$[\upsilon]^{-1}\left(\frac{\tilde{\Phi}^{(\tau+1)}-\tilde{\Phi}^{(\tau)}}{\Delta t}\right)=-[B]^{(\tau+1)}\tilde{\Phi}^{(\tau+1)}+(1-\beta)[F]^{(\tau+1)}\tilde{\Phi}^{(\tau+1)}+[S]^{(\tau+1)}\tilde{\Phi}^{(\tau+1)}+\sum_{l=1}^{6}\lambda_l\,\tilde{\varsigma}_l^{(\tau+1)}+\tilde{S}_{es}^{(\tau)}\quad . \tag{9}$$

Replacing Equation (7) in Equation (9) the result is the following system of linear equations:

$$\begin{bmatrix}T_{11} & T_{12}\\ T_{21} & T_{22}\end{bmatrix}\begin{pmatrix}\tilde{\phi}_1\\ \tilde{\phi}_2\end{pmatrix}^{(\tau+1)}=\begin{bmatrix}R_{11} & R_{12}\\ 0 & R_{22}\end{bmatrix}\begin{pmatrix}\tilde{\phi}_1\\ \tilde{\phi}_2\end{pmatrix}^{(\tau)}+\upsilon_1\Delta t\sum_{l=1}^{L}\lambda_l e^{-\lambda_l\Delta t}\begin{pmatrix}\tilde{\varsigma}_l\\ \tilde{0}\end{pmatrix}^{(\tau)}+\begin{pmatrix}\upsilon_1\Delta t\tilde{S}_{se,1}\\ \upsilon_2\Delta t\tilde{S}_{se,2}\end{pmatrix}^{(\tau)} \tag{10}$$

where the blocks of matrix are given for:

$$[T_{11}]=[I]+\upsilon_1\Delta t\left([B_1]^{(\tau+1)}-\left((1-\beta)+\sum_{l=1}^{L}\lambda_l\beta_l b_l\right)[F_{11}]^{(\tau+1)}\right), \tag{11}$$

$$[T_{12}]=-\upsilon_1\Delta t\left((1-\beta)+\sum_{l=1}^{L}\lambda_l\beta_l b_l\right)[F_{12}]^{(\tau+1)}, \tag{12}$$

$$[T_{21}]=-\upsilon_2\Delta t[S_{21}]^{(\tau+1)}, \tag{13}$$

$$[T_{22}]=[I]+\upsilon_2\Delta t[B_2]^{(\tau+1)}, \tag{14}$$

$$[R_{11}]=[I]+\upsilon_1\Delta t\sum_{l=1}^{L}\lambda_l\beta_l a_l[F_{11}]^{(\tau)}, \tag{15}$$

$$[R_{12}]=\upsilon_1\Delta t\sum_{l=1}^{L}\lambda_l\beta_l a_l[F_{12}]^{(\tau)}, \tag{16}$$

$$[R_{22}]=[I]. \tag{17}$$

3. RESULTS

3.1. Validation of Numerical Method

To validate the developed codes, a homogeneous cubic core with 200 cm of edge, without reflector, with two groups of energy and one group of precursors [10]. Nuclear material properties and kinetic data are given in Table 1. The spatial discretization in finite differences adopted was $\Delta x = \Delta y = \Delta z = 10$ cm, with twenty radial planes, each plane with 400 boxes, totaling 8000 boxes. A mesh size of 10 cm is allowed, as the diffusion length for this reactor is 14 cm. In the steady-state calculation a $k_{eff.} = 0.893508$ is found which corresponds to a percentage relative deviation of 0.002% when compared to the exact value (0.895285). In the simulation of the transient was considered a uniform step disturbance, where the absorption cross section in the thermal group is decreased by a value of 0.369×10^{-4} cm^{-1}. The transient lasted 0.4 s and a temporal discretization was adopted with $\Delta t = 0.001s$. In Table 2 the results obtained by the code are compared with the exact solution that can be found in [10]. The comparison is made with the thermal flux at the core center, where at the initial time it is normalized to the unit (second column). It is verified that the percentage relative deviation is less than 1% during the transient.

Table 1: Homogenous reactor - nuclear and kinetic parameters.

Type	***g***	D_g ***(cm)***	$\sum_{ag}$ ***(cm)$^{-1}$***	$\nu\sum_{fg}$ ***(cm)$^{-1}$***	$\sum_{gg'}$ ***(cm)$^{-1}$***	υ_g ***(cm/s)***
1	1	1.35062	0.001382	0.00058322	0.0023	3.0×10^7
	2	1.08085	0.0054869	0.0098328	0.0	2.2×10^5

$\lambda_1 = 0.08s^{-1}$, $\beta_1 = 0.0064$
$\nu = 2.41 neutrons/fission$

Table 2: Homogenous reactor – comparison of the calculated normalized thermal flux at the core center with exact solution (Ref. 10).

Time (s)	**Exact**	**Calculate**	**Deviation (%)**
0.00	1.0000	1.0000	-
0.10	1.7243	1.7167	0.44
0.20	2.3162	2.3077	0.37
0.30	2.8039	2.7949	0.33
0.40	3.2108	3.2015	0.29

In Figures 1 and 2 are shown the fast and thermal fluxes at the central plane of the homogeneous core at the initial time and Figures 3 and 4 show the fast and thermal fluxes at the final instant.

Figure 1: *Fast Neutron Flux, t = 0s.*

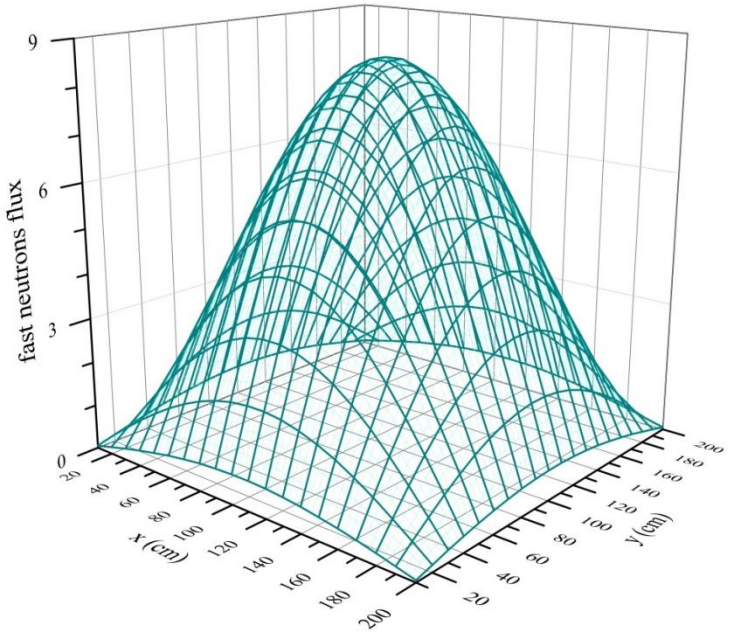

Figure 2: *Thermal Neutron Flux, t = 0s.*

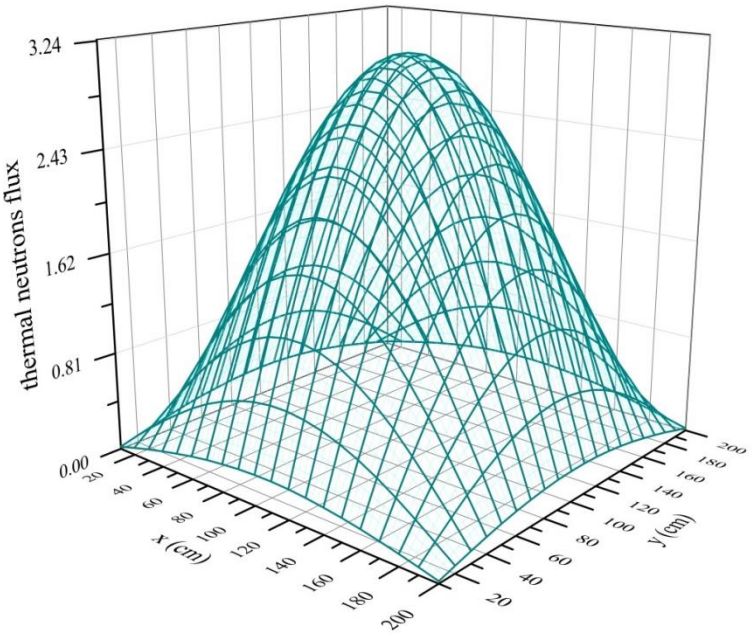

Figure 3: *Fast Neutron Flux, t = 4s.*

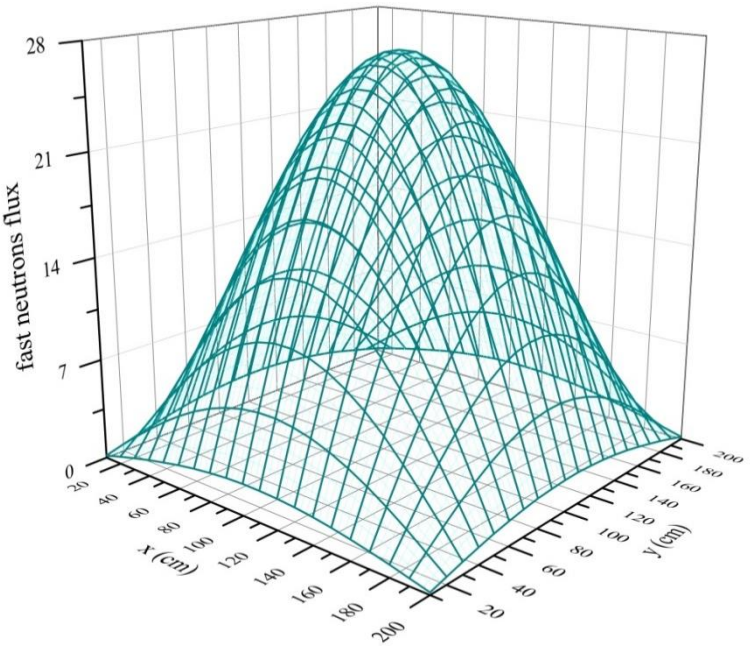

Figure 4: *Thermal Neutron Flux, t = 4s.*

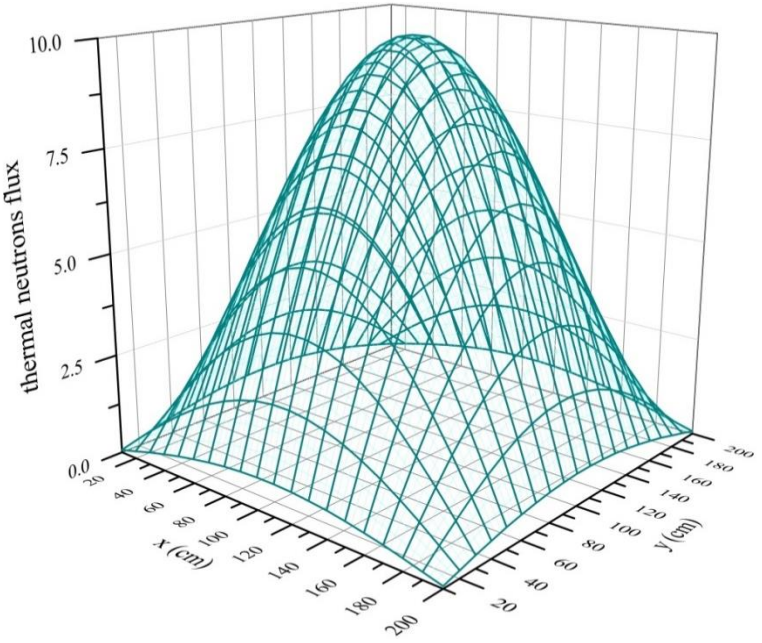

3.2. Analysis of Transients in an ADS-3D

In this section, the Implicit Euler method was used to analyze some types of transients caused by the external neutron source in a tree-dimensional ADS reactor. The tree-dimensional ADS

reactor has its geometry and diffusion kinetic parameters similar to the core shown in sect. 3.1. The external neutron source is located in the center of the reactor and being in the form of a small cube of 20 cm of edge. This source of neutrons, which represents the source of spallation that is bombarded by the proton beam, can be approximated as a source of constant intensity because the proton beam employed in ADS reactors is produced by continuous waves that operates at a very high frequency, above 170 MHz. In the cases of transients that will be approached in the next sections, an external neutron source with a constant intensity equal to 10^{14} neutrons/s was adopted.

3.2.1 Methods and Data

Using the codes, two types of transients associated with an ADS reactor will be simulated and will focus on the proton accelerator perturbations, causing variations in the intensity of the proton beam and consequently the intensity of the external source of neutrons. The first transient corresponds to the interruption in the proton beam for a short period of time and the second transient to be addressed describes the occurrence of a power peak in the proton beam [2], [3], [4], [5]. In order to simulate the transients, the same spatial and temporal discretization of the previous section was considered.

3.2.1.1. Accelerator beam interruption (ABI)

In this transient the reactor is operating critically and the proton beam of the accelerator is interrupted in the instant in 1 s and after 2 s over the beam is reconnected. Fig. 5 and Fig. 6 illustrate the behavior of the fast and thermal neutron fluxes at the instant in 1 s, at the beginning of the ABI, and Fig. 7 and Fig. 8 show the fast and thermal neutron fluxes at the instant in 3 s, at the end of the ABI. Fig. 9 shows the behavior of the relative power, considering a simulation with the duration of 10 s. With the interruption of the proton beam at the instant in 1 s an abrupt change in power is observed, with a 94% reduction in 0.04s, and also an abrupt change occurs throttle drive in 3 s. It is also observed that between these instants, the power is reduced slowly due to the sub-criticality of the ADS reactor. The results obtained in the simulation of the ABI are very similar to those obtained in simulations of the ABI using a slab type reactor [4], [5] and also in simulations considering a reactor in two-dimensional geometry [2], [3].

Figure 5: *Case ABI - Fast Neutron Flux, t = 1s.*

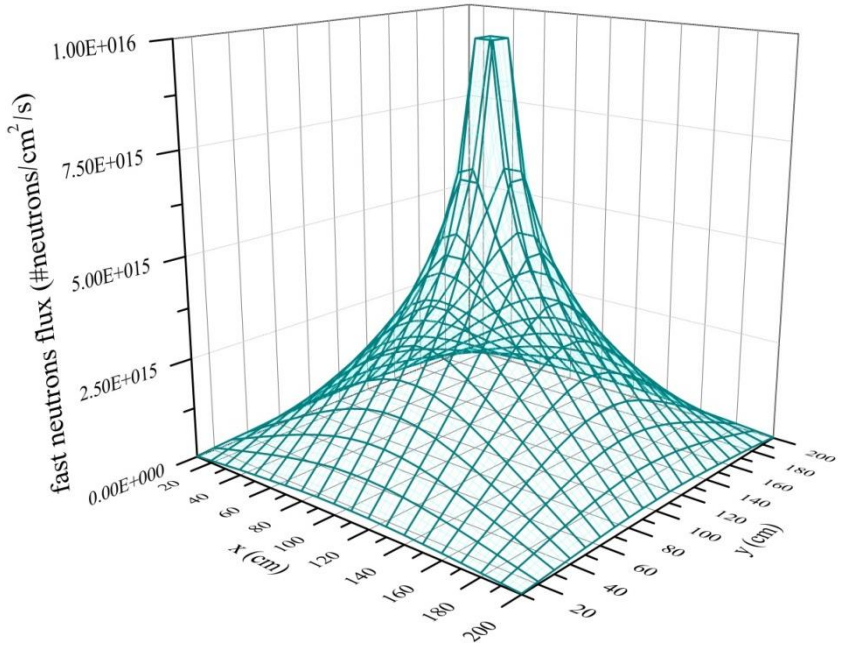

Figure 6: *Case ABI - Thermal Neutron Flux, t = 1s.*

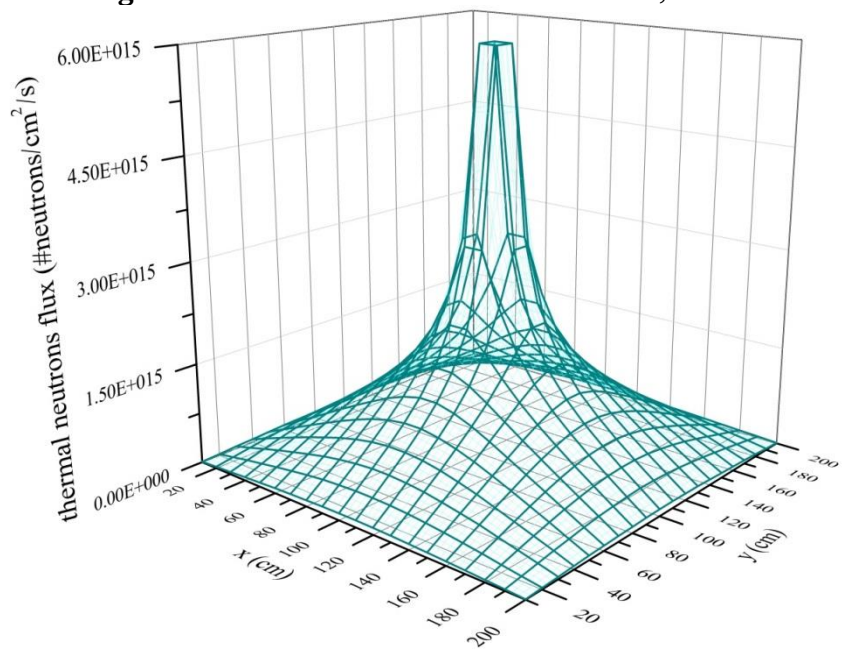

Figure 7: *Case ABI - Fast Neutron Flux, t = 3s.*

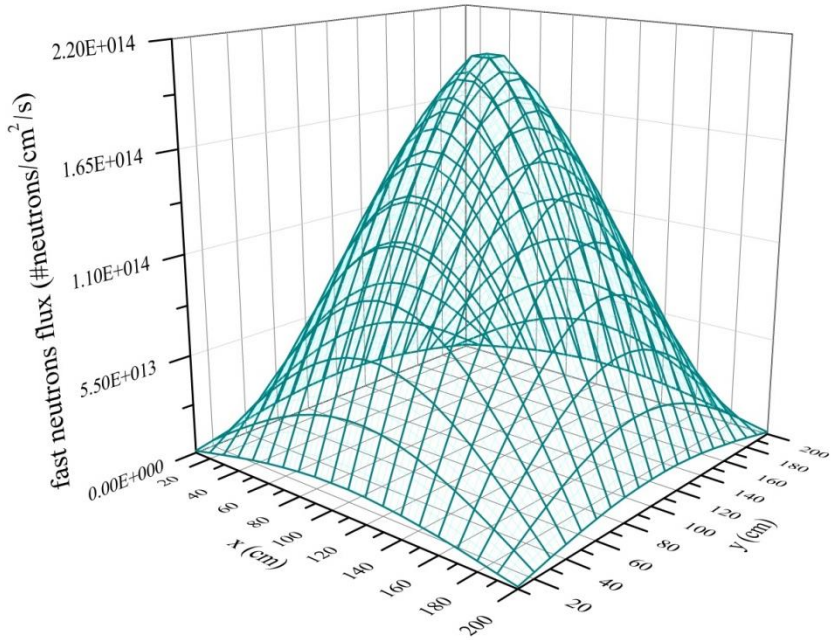

Figure 8: *Thermal Neutron Flux, t = 3s.*

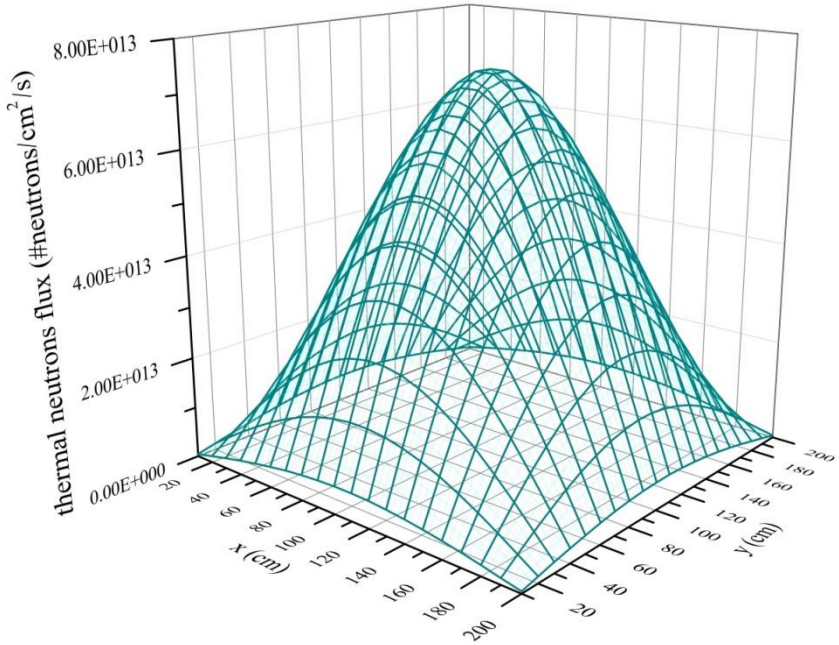

Figure 9: *Case ABI - Relative Power variation.*

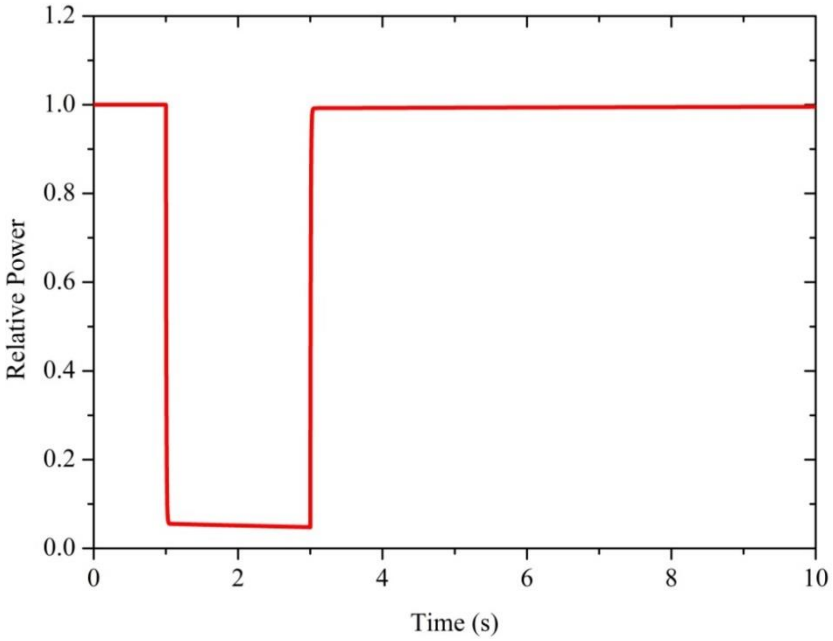

3.2.1.2. Accelerator beam over-power (ABO)

In this transient the reactor is operating critically and the intensity of the proton beam of the accelerator is increased by 100% instantaneously and after 2 s over the beam has its intensity restored to the initial level. Fig. 10 and Fig. 11 show the fast and thermal neutron fluxes at the instant in 3 s, at the end of ABO. The behavior of the relative power in the transient ABO, considering a simulation with the duration of 10 s can be verified in Fig. 12. With the increase in the intensity of the proton beam of the accelerator in the instant in 1 s an instantaneous variation of the relative power is observed, with an increase of 94% in 0.04s. With the accelerator operating at normal intensity, the ADS reactor operates at criticality and therefore, with an increase in beam intensity, the reactor starts operating on super-criticality. Thus, a gradual increase in power between the instants of 1 s and 3 s can be observed.

In the same way as in the ABI case, the results obtained in the simulation of the ABO transient are very similar to the results obtained in the simulations of ABO in slab type reactors [4], [5] and in reactors in two-dimensional geometry [2], [3].

Figure 10: *Case ABO - Fast Neutron Flux, t = 3s.*

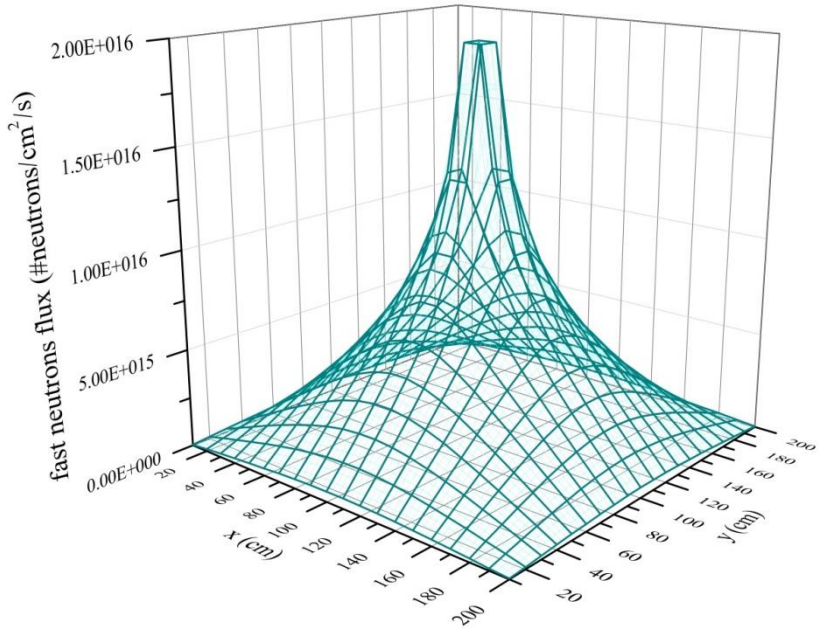

Figure 11: *Case ABO - Thermal Neutron Flux, t = 3s.*

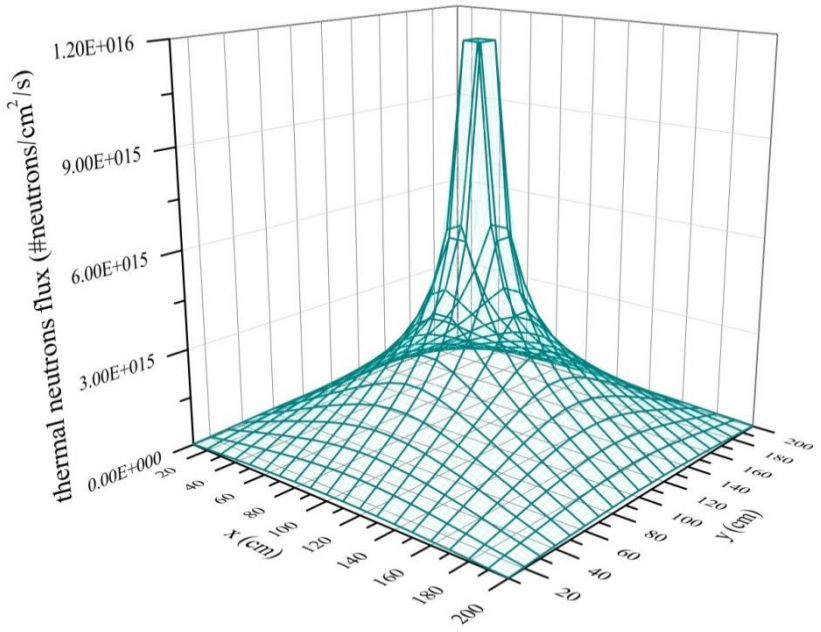

Figure 12: *Case ABO - Relative Power variation.*

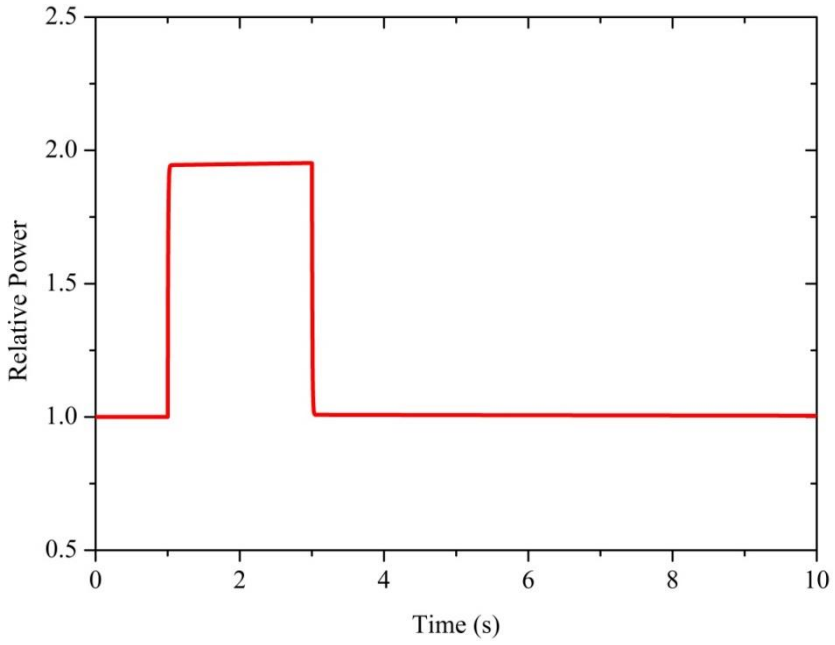

4. CONCLUSIONS

In this work, the spatial kinetics equations were modeled numerically to obtain the neutron flux distribution and the power of a three-dimensional nuclear reactor. The delayed neutron precursor equation was integrated analytically and the numerical method to discretize spatial kinetics equations was finite differences. The dependence in time was solved by the well-known implicit Euler method. The computational code of the numerical implementation was programmed in the Fortran language. The code was validated considering a transient simulation in a three-dimensional homogeneous reactor for two energy groups and one group of precursors of delayed neutrons. Then the code was tested to simulate transients of an ADS, whose geometry and composition are the same as the reactor core used in the validation, differing only with the presence of an intense source of neutrons in its center, representing the source of spallation due to the action of a proton accelerator. Two transients associated with variations in neutron source intensity were simulated: Accelerator beam interruption and Accelerator beam over-power. Although there are no other results in the literature to make a comparison, the results obtained are very similar to those obtained in simulations using a slab-type reactor and in two-dimensional geometry. Continuing this study, the code will be tested in three-dimensional reactor cores with more than one region and six groups of precursors.

ACKNOWLEDGMENTS

The authors are grateful for the support provided by the Comissão Nacional de Energia Nuclear (CNEN), Brazil.

REFERENCES

[1] C. RUBBIA, et al. **Conceptual Design of a Fast Neutron Operated High Power Energy Amplifier**, CERN Report, CERN/AT/95-44 (ET), Genebra (1995).

[2] A.J. FIGUEIRA, A.C.M. Alvim and F.C. da Silva, **Non Symmetric Alternating Direction Explicit Method Applied to the Calculation of ADS Transients**, Annals of Nuclear Energy, 90, pp.459-467 (2016). http://dx.doi.org/10.1016/j.anucene.2015.11.016

[3] A. J. FIGUEIRA, **Cinética Espacial para Modelar Transientes em Reatores ADS**, tese de Doutorado, PEN-COPPE-UFRJ, Rio de Janeiro, Brazil (2015).

[4] W. V. de ABREU, A. C. GONÇALVES, Z. R. de LIMA, **Numerical Analysis for Transients in External Source Driven Reactors**, World Journal of Nuclear Science and Technology, 07, pp.103-120 (2017).

[5] W. V. de Abreu, **Análise Numérica de Transientes em um Reator Slab Guiado por Fonte Externa**, Dissertação de Mestrado, IEN-CNEN, Rio de Janeiro, Brazil (2017).

[6] S. NAKAMURA, **Computational Methods in Engineering and Science**, Wiley and Sons, New York, USA (1977).

[7] A.C.M. ALVIM, **Métodos Numéricos em Engenharia Nuclear**, 1th Edition, Certa Ltd., Curitiba, Brazil (2007).

[8] W.M. STACEY, **Space-Time Nuclear Reactor Kinetics**, Academic Press, New York, USA (1969).

[9] H.W. PRESS, S.A. TEUKOLSKY, W.T. VETTERLING, et al. **Numerical Recipes in Fortran**, 2th Edition, Cambrige University Press, New York, USA (1992).

[10] D. R. FERGUSON & K. F. HANSEN, **Solution of the Space-Dependent Reactor Kinetics Equations in Three Dimensions**, Nuclear Science and Engineering, 51:2, pp.189-205 (1973).